Journal of Bioenergetics and Biomembranes, Vol. 24, No. 3, 1992

Structural Features of Cation Transport ATPases

Giuseppe Inesi[1] and Mary R. Kirtley[1]

Received February 23, 1992; accepted February 25, 1992

Several cation transport ATPases, sharing the common feature of a phosphorylated intermediate in the process of ATP utilization, are compared with respect to their subunit composition and amino acid sequence. The main component of these enzymes is a polypeptide chain of MW slightly exceeding 100,000, comprising an extramembranous globular head which is connected through a stalk to a membrane-bound region. With reference to the Ca^{2+} ATPase of sarcoplasmic reticulum, it is proposed that the catalytic (ATP binding and phosphorylation) domain resides in the extramembranous globular head, while cation binding occurs in the membrane region. Therefore, these two functional domains are separated by a distance of approximately 50 Å. Alignment of amino acid sequences reveals extensive homology in the isoforms of the same ATPases, but relatively little homology in different cation ATPases. On the other hand, all cation ATPases considered in this analysis retain a consensus sequence of high homology, spanning the distance between the phosphorylation site and the preceding transmembrane helix. It is proposed that this sequence provides long-range functional linkage between catalytic and cation-binding domains. Thereby, translocation of bound cation occurs through a channel formed by transmembrane helices linked to the phosphorylation site. Additional sequences at the carboxyl terminal provide regulatory domains in certain ATPases.

KEY WORDS: Cation transport; Ca^{2+}, ATPase; Na^+, K^+, ATPase; H^+, ATPase; structure–function relationships; transport mechanism.

INTRODUCTION

The P-type cation-transport ATPases are membrane-bound enzymes consisting of a main polypeptide chain of approximately 110,000 MW, which is the sole or principal operator of both catalytic and transport functions. Additional subunits or dimerization of the main polypeptide chain occur in some cases (Table I). The 110,000 MW chain includes a relatively large extramembranous domain and a number (eight or ten) of transmembrane helical segments which penetrate the membrane bilayer and return to the extramembranous domain in the form of (four or five) hairpins. Another, common structural feature is the presence of an aspartyl residue which is the specific acceptor of ATP terminal phosphate for formation of a covalent intermediate (E-P) during the catalytic cycle. Our aim in this article is to identify structural features involved in general catalysis, specific cation binding, and coupling of catalytic and transport functions in the main polypeptide unit. To this aim, we compare the structural features of various cation ATPases and their isoforms, with reference to the Ca^{2+}-ATPase. More detailed analysis of structure and function relationships can be found in Inesi and Kirtley (1990), Inesi *et al.* (1990), Kirtley and Inesi (1992), and Inesi *et al.* (1992).

SEQUENCES AND TOPOLOGY

Early sequencing efforts on accessible peptide segments were followed by cloning and sequencing of full-length *c*DNAs encoding various cation ATPases.

[1]Department of Biological Chemistry, University of Maryland School of Medicine, Baltimore, Maryland 21201.

0145-479X/92/0600-0271$06.50/0

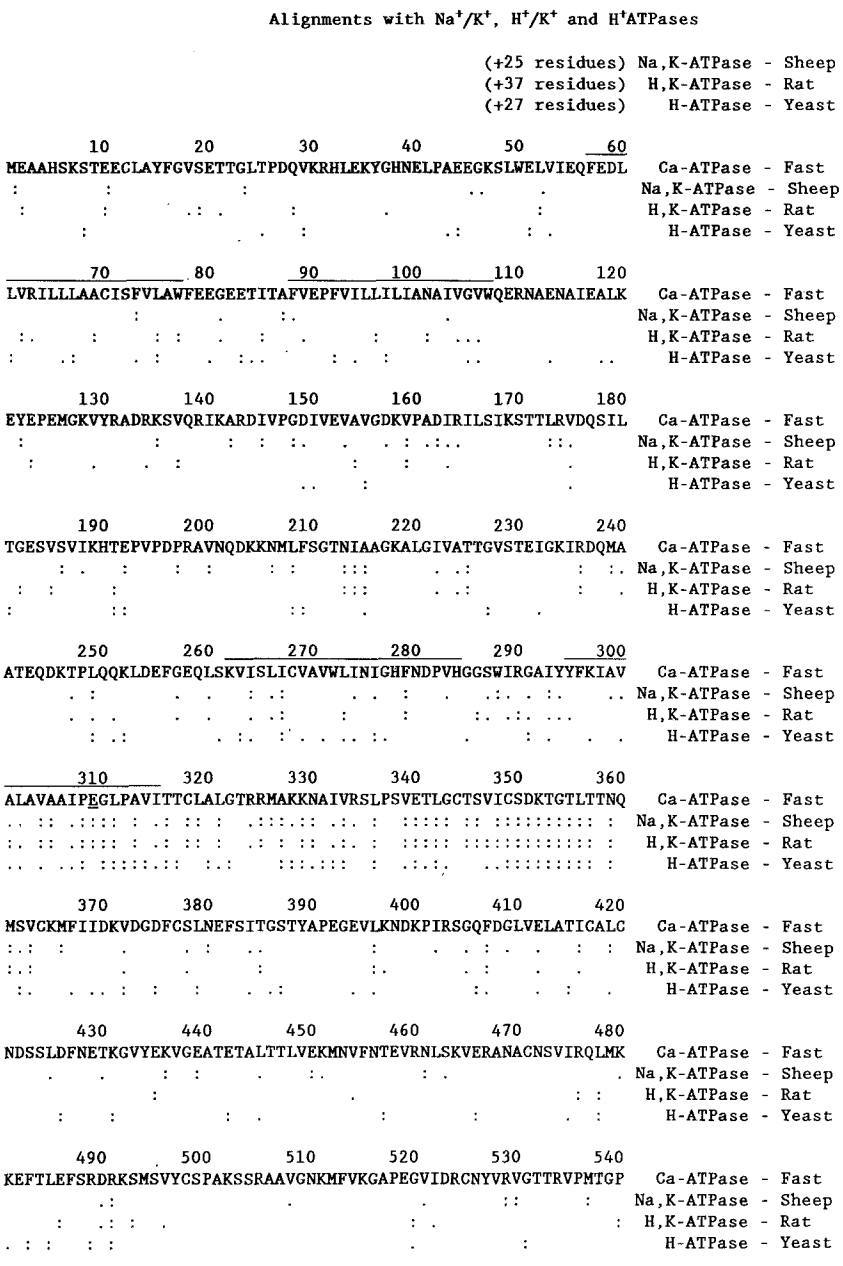

Fig. 1. Comparison of the sequence of Ca^2-ATPase of skeletal muscle with sequences of other transport ATPases. The sequence shown is that of the fast Ca^{2+}-ATPase of sarcoplasmic reticulum. Identical (:) or related (.) residues in the other proteins are indicated. Blank spaces indicate unrelated amino acid residues in those positions. / = start of sequence; \ = end of sequence; —— = Transmembrane segment [Clarke *et al.* (1989 model)]. Where a sequence extends beyond that of the Ca^{2+}-ATPase, the number of additional residues is shown in parentheses. The residues associated with calcium binding are underlined. Note that all of these are retained in the slow Ca^{2+}-ATPase, only two of them are retained in the erythrocyte Ca^{2+}-ATPase, and only one appears in the other ATPases. The various enzymes are denoted as follows: Ca-ATPase—fast = calcium-transporting ATPase, fast twitch skeletal muscle—rabbit (Brandl *et al.*, 1986); Na,K-ATPase—sheep = sodium/potassium-transporting ATPase, alpha chain precursor–sheep (Shull *et al.*, 1985); H,K-ATPase—rat = proton/potassium ATPase—rat (Maeda *et al.*, 1888, 1990) H-ATPase–yeast = proton-transporting ATPase–yeast (*Saccharomyces sp.*) (Serrano *et al.*, 1986).

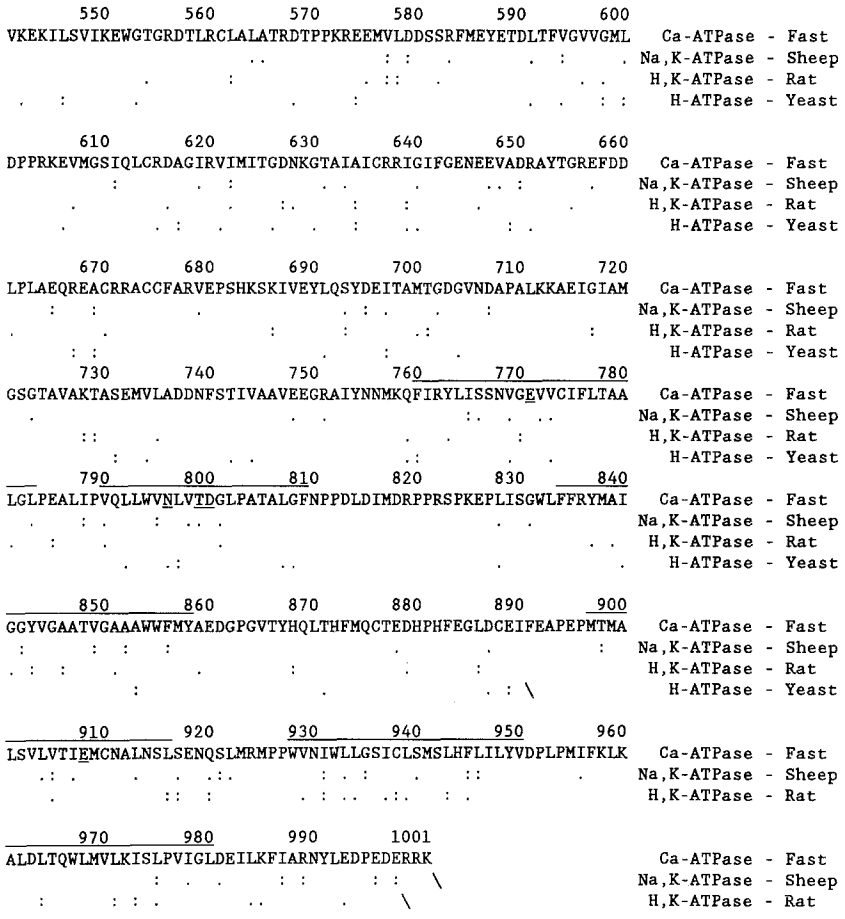

Fig. 1. Continued.

Table I. Composition of Major Subunits of Intracellular Ca^{2+}-ATPase, Plasma Membrane Ca^{2+}-ATPase, Na^+, K^+-ATPase, and H^+, K^+-ATPase

	Subunit	Subunit molecular weight	Function	References
Ca^{2+}-ATPase intracellular (SERCA1)	Main chain	110,458 (may form dimers)	Ca^{2+} pump	Brandl *et al.* (1986)
Ca^{2+}-ATPase plasmalemmal (erythrocyte)	Main chain	134,709	Ca^{2+} pump	Verma *et al.* (1988)
Na^+, K^+-ATPase, sheep	Alpha Beta	112,657 35,061	Na^+, K^+ pump structural	Shull *et al.* (1985) Kawakami *et al.* (1986)
H^+, K^+-ATPase rat	Alpha Beta	114,286 33,419	H^+, K^+ pump structural	Maeda *et al.* (1988) Maeda *et al.* (1990) Renben *et al.* (1990)

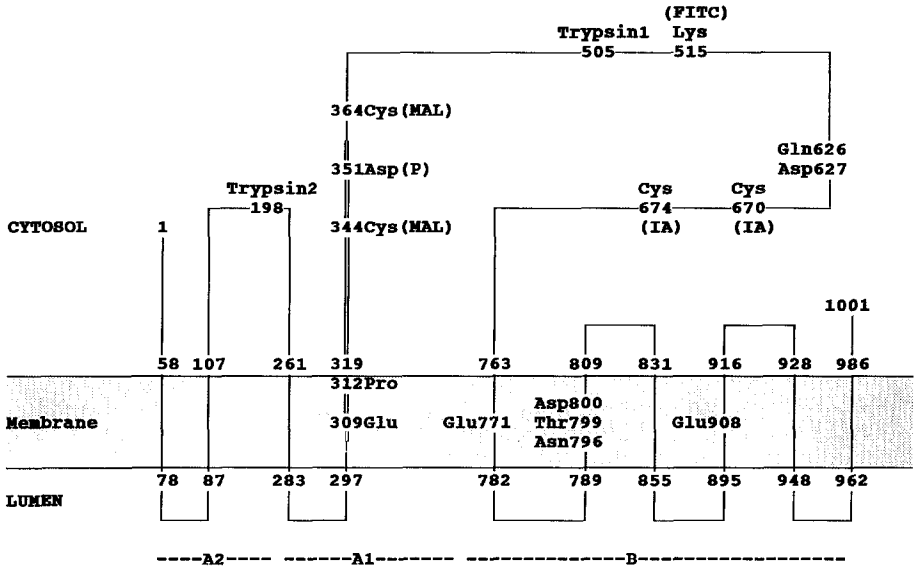

Fig. 2. Topology of the Ca^{2+}-ATPase in the sarcoplasmic reticulum membrane. Large segments at the top extend into the cytosol; short segments are exposed at the lumenal side of the membrane. The model shown is based on that of Clarke *et al.* (1989). Asp351 undergoing phosphorylation is shown in the extramembranous region. Residues Glu309, Glu771, Asp800, Thr799, Asn796, and Glu908, involved in Ca^{2+} binding functions, are shown in the membrane region. The double line denotes the consensus sequence in many cation transport ATPases, linking the phosphorylation and calcium-binding domains. The sites of trypsin digestion are shown, and the resulting peptides are denoted A2, A1, and B at the bottom of the figure. Cysteine residues reactive with maleimide (MAL) or iodacetamide (IA) derivatives are shown, as is the site for FITC reaction which interferes with ATP binding to the enzyme. Gln626 and Asp627, as well as Asp351, when mutated, result in loss of catalytic activity.

In Fig. 1 we are comparing the amino acid sequence of the fast muscle sarcoplasmic reticulum (SR) ATPase to three other ATPases sustaining transport of different cations in mammalian and yeast cells. The fast muscle SR ATPase consists of 1001 amino acids in a single polypeptide chain. Hydropathy analysis of this sequence suggests that ten segments (identified by a solid line in Fig. 1) fold as transmembrane helices crossing the membrane ten times in the shape of five hairpins (Fig. 2).Thereby both amino and carboxyl terminals remain on the cytosolic side of the membrane, and a large portion of the polypeptide chain is outside the membrane, and a large portion of the polypeptide chain is outside the membrane on the cytoplasmic side (Fig. 2).

Alignment with other cation ATPases (Fig. 1) shows little homology, except for a segment intervening between residues 308 and 358 in the SR ATPase. This segment includes Asp351, which is the residue undergoing phosphorylation for formation of the catalytic intermediate (Yamamoto and Tonomura, 1968; Makinose, 1969), and a preceding sequence connecting this segment to the fourth transmembrane helix. In analogy to the SR ATPase, hydropathy analysis of the other sequences singles out eight or ten segments that are likely to be assembled as transmembrane helices.

CATALYTIC AND CATION BINDING SITES

A most important lead to localization of the catalytic site within the ATPase molecule was the identification of a specific aspartyl residue (351 in the SR Ca^{2+}-ATPase) undergoing phosphorylation as an intermediate step of the catalytic cycle (Bastide *et al.*, 1973; Degani and Boyer, 1973). Furthermore, the interference of specific amino acid derivatization with ATP binding (Mitchinson *et al.*, 1982), as well as considerations of homology with adenyl kinase and phosphoglycerate kinase (Taylor and Green, 1989), indicate that the catalytic and ATP binding sites reside in the extramembranous domain of the cation-transport ATPases.

Localization of the cation-binding sites proved to be more difficult. Nevertheless, for the SR Ca^{2+}-ATPase, site-directed mutagenesis (Clarke *et al.*,

Table II. Isoforms of Ca^{2+}-ATPases

Isoform	Source	Molecular weight	References
	Organellar Ca^{2+}-ATPases		
SERCA1			
Rabbit	Skeletal muscle SR	110,458	Brandl *et al.* (1986)
Chicken	Skeletal muscle SR	109,034	Karin *et al.* (1989)
Brine shrimp	Muscle SR	110,343	Palmero and Sastre (1989)
SERCA2a			
Rabbit	Cardiac SR	109,643	MacLennan *et al.* (1985)
Chicken	Cardiac SR, slow twitch ER	109,700	Campbell *et al.* (1991)
Human	Kidney ER	109,690	Lytton and MacLennan (1988)
Pig	Smooth muscle ER	109,725	Eggermont *et al.* (1989, 1990)
Rat	Brain, stomach, kidney ER	109,680	Gunteski-Hamblin *et al.* (1988)
Rat	Cardiac SR, slow skeletal SR	109,537	Lompre *et al.* (1989)
SERCA2b			
Human	Kidney ER	114,756	Lytton and MacLennan (1988)
Chicken	Brain ER, cardiac ER	~115,000	Campbell *et al.* (1991)
Rabbit	Smooth muscle SR	114,705	Lytton *et al.* (1989)
Pig	Smooth muscle ER	114,791	Eggermont *et al.* (1989, 1990)
Rat	Brain, stomach, kidney ER	114,767	Gunteski-Hamblin *et al.* (1988)
SERCA3			
	Brain ER, skeletal muscle SR		Greeb and Shull (1989)
		109,336	Burk *et al.* (1989)
	Plasmalemmal Ca^{2+}-ATPases		
PMCA1			
Human	Erythrocyte plasma membrane	134,709	Verma *et al.* (1988)
Rat	Brain plasma membrane	129,509	Shull and Greeb (1988)
PMCA2			
Human	Erythrocyte plasma membrane	133,930	Strehler *et al.* (1989, 1990)
Rat	Brain plasma membrane	132,615	Shull and Greeb (1988)
PMCA3			
Rat	Brain, skeletal muscle plasma membrane	127,296	Shull and Greeb (1988) Greeb and Shull (1989)
PMCA4			
Human	Muscle plasma membrane	~144,000	Shrehler *et al.* (1989)
Human	Muscle plasma membrane	~145,000	Strehler *et al.* (1989)

1989a) and chemical derivatization (Sumbilla *et al.*, 1991) suggest that Ca^{2+} binding involved in catalytic activation and transport occurs within the membrane domain, at a considerable distance from the catalytic site. Specific residues whose mutation interferes with Ca^{2+} binding functions are Glu309, Glu771, Asp800, Thr799, Asp796, and Glu908 (Fig. 2).

ENZYME ISOFORMS

For the same type of cation-transport ATPase (e.g., intracellular Ca^{2+}-ATPase, plasma membrane Ca^{2+}-ATPase, Na^+,K^+-ATPase), various isoforms resulting from alternate splicing of the primary RNA transcript have been described (Table II) The sequences of five intracellular Ca^{2+}-ATPase isoforms are aligned in Fig. 3 and compared to the erythrocyte plasma membrane Ca^{2+}-ATPase. The extensive homology of the isoforms is obvious, as is the interesting low degree of homology with the plasma Ca^{2+}-ATPase (except for the phosphorylation site segment). The membrane domain residues involved in Ca^{2+} binding are all conserved in the intracellular Ca^{2+}-ATPase isoforms, while only two are retained in the plasma membrane Ca^{2+}-ATPase. It is of interest that the human erythrocyte plasma membrane Ca^2-ATPase and the SERCA2aCa^{2+}-ATPase sequences show carboxyl and

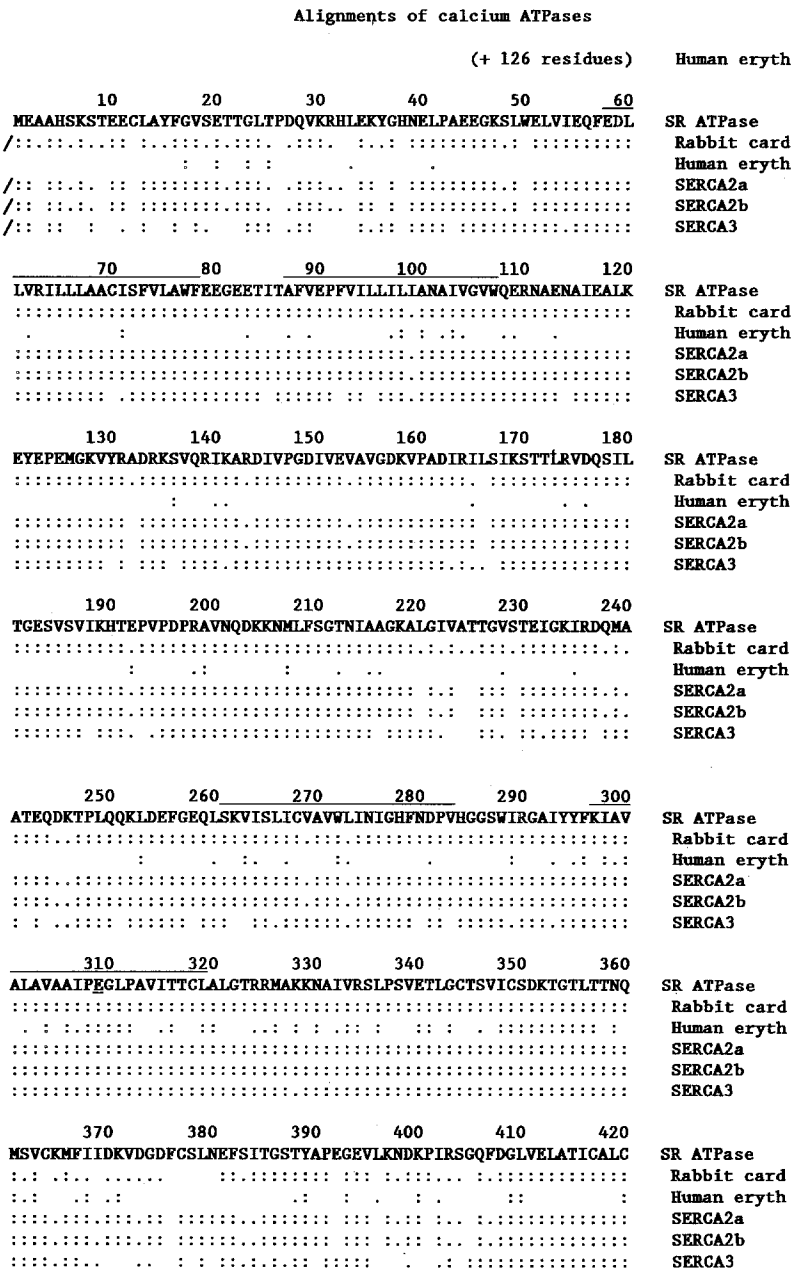

Fig. 3. Comparison of the sequence of SR Ca^{2+}-ATPase of skeletal muscle with sequences of other calcium-transporting ATPases. The sequence shown is that of the SR Ca^{2+}-ATPase. Identical (:) or related (·) residues in the other proteins are indicated. Blank spaces indicate unrelated amino acid residues in those positions. \ = Start of sequence; \ = End of sequence; ■—■ = Transmembrane segment (Clarke *et al.*, (1989). Where a sequence extends beyond that of the SR-Ca^{2+}-ATPase, the number of additional residues is shown in parentheses. The residues associated with calcium binding are shown underlined. Note that all of these are retained in the slow Ca-ATPase and, only two of them are retained in the erythrocyte Ca-ATPase. The various enzymes are denoted as follows: SR ATPase = calcium-transporting ATPase, fast twitch skeletal muscle from rabbit (Brandl *et al.*, 1986); rabbit card = calcium-transporting ATPase, slow twitch skeletal muscle from rabbit (MacLennan *et al.*, 1985); human eryth = calcium-transporting ATPase, erythrocyte membrane from human (Verma *et al.*, 1988); SERA2a = chicken cardiac and slow twitch skeletal muscle Ca^{2+}-ATPase (Campbell *et al.*, 1991); SERCA2b = chicken brain endoplasmic reticulum Ca^{2+}-ATPase (Campbell *et al.*, 1991); SERCA3 = rat "organellar" Ca^{2+} pump (Burk *et al.*, 1989).

Fig. 3. Continued.

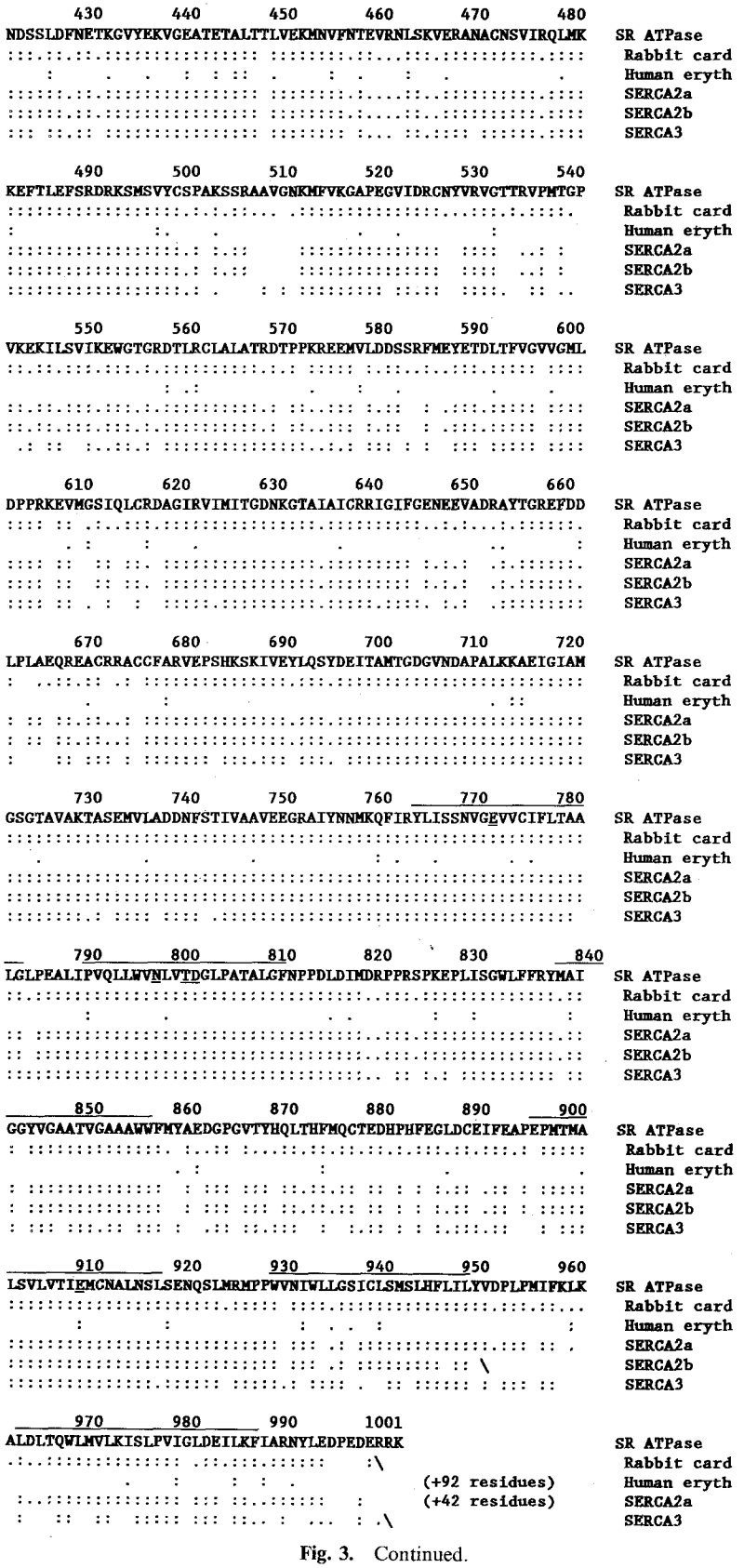

Fig. 3. Continued.

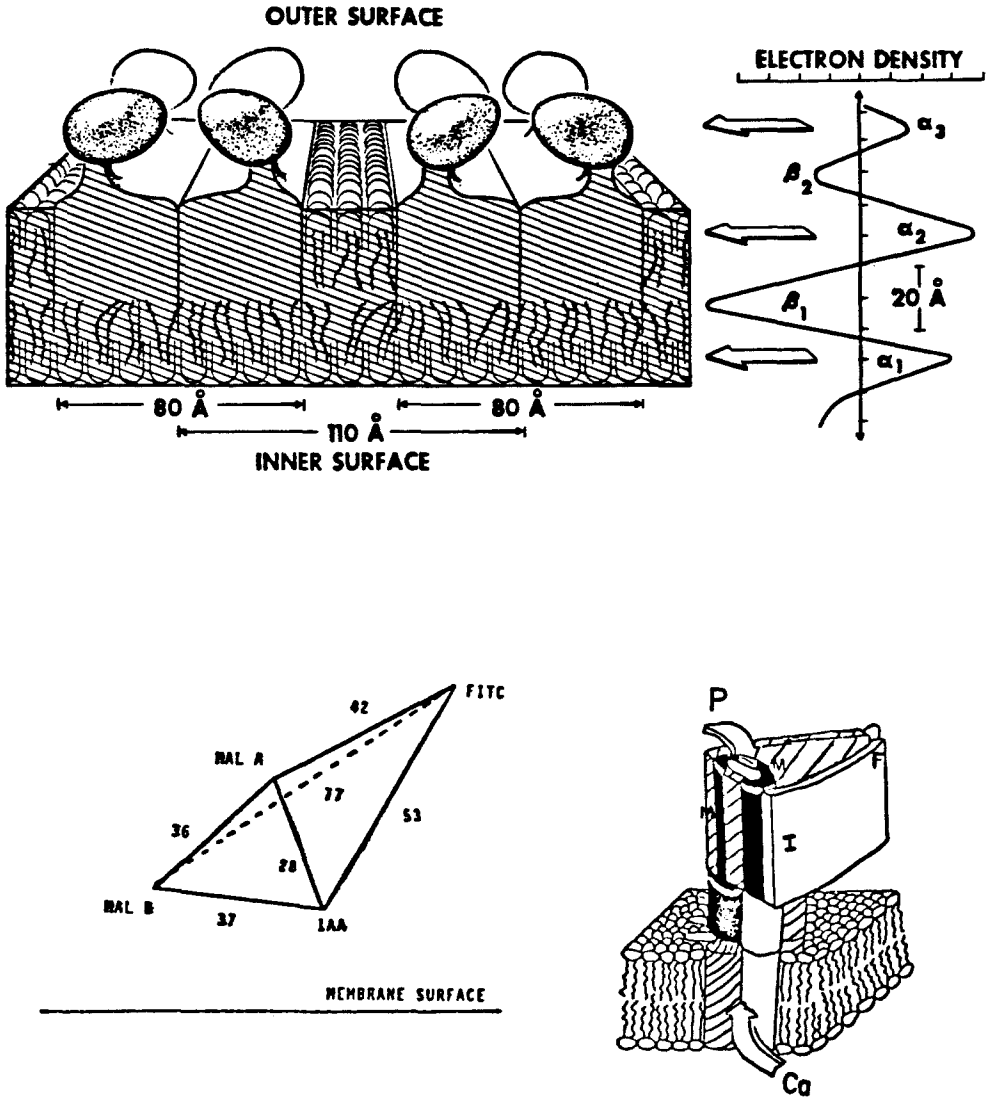

Fig. 4. Shape and membrane assembly of the SR Ca^{2+} ATPase. Top: A diagram based on early electron microscopic observations represents the dense distribution of the enzyme on the SR membrane, and its tendency to form oligomeric arrays (Inesi, 1979). A pear-shaped globular region on the cytoplasmic ("outer" in the vesicles) side of the membrane is connected through a stalk with a membrane-bound region. A matching electron density distribution along the axis perpendicular to the membrane plane was derived from x ray diffraction of stacked membranes (Dupont *et al.*, 1973). Bottom: Model of spatial relationships of fluorescent labels of the Ca^{2+}-ATPase (Bigelow and Inesi, 1991). The diagram on the left side depicts a fluorescent isothiocyanate label of Lys515 (FITC), the iodoacetamide-directed labels of Cys670, 674 (IAA), and the maleimide-directed labels of Cys 344 and Cys364 (MAL A and B). The numbers indicate the mean distances in angstroms, as derived from estimate of fluorescence resonance energy transfer. The diagram on the right side portrays a cartoon model for the three-dimensional folding of the ATPase, which attempts to reconcile the predicted folding of the sequence (MacLennan *et al.*, 1985) with the topology of the enzyme derived from electron microscopy and diffraction data (Castellani *et al.*, 1985; Taylor *et al.*, 1986; Stokes and Green, 1990), and the spatial relationship of fluorescent labels derived from spectroscopic studies (Squier *et al.*, 1987; Bigelow and Inesi, 1991). The cytoplasmic head of the enzyme forms a trigonal arrangement with the B (white) tryptic fragment folded over the A1 (hatched) and A2 (solid black) fragments to form a crevice including the catalytic site (P for phosphorylation domain). The FITC-, iodoacetamide-, and maleimide-directed labels are shown by the letters F, I, and M, respectively. The cylinder depicts the stalk and transmembrane helices in clustered configuration, including the Ca^{2+} binding domain (Ca). The model is scaled to be consistent with a membrane thickness of 40 Å, a 40 × 50 × 65 Å head centered 35 Å above the membrane bilayer, and a 28 Å diameter stalk that extends 16 Å from the membrane bilayer.

extensions of 92 and 48 residues, respectively (Fig. 3). These extensions include two calmodulin binding sites and, in the case of PMCA2 from rat brain (Shull and Greeb, 1988; James *et al.*, 1989) the site of phosphorylation by *c*AMP protein kinase. These sites are likely to be related to enzyme regulation by calmodulin in the plasma membrane Ca^{2+}-ATPase, or other ligands such as phospholamban in the SERCA2a (cardiac) ATPase.

SHAPE AND FOLDING OF THE SR Ca^{2+}-ATPase

Owing to its natural abundance and dense spacing on the plane of the membrane, as well as its homogeneous polypeptide composition, the SR Ca^{2+}-ATPase has been studied more extensively than other cation ATPases. A globular region protruding from the cytoplasmic side of the membrane connected through a stalk to a membrane region, and minimal protein extension on the lumenal surface of the membrane, was already noted by early electron microscopic observations (Inesi and Asai, 1968; Deamer and Baskin, 1969). Such a disposition of the protein mass was subsequently confirmed by wide-angle x-ray (Dupont *et al.*, 1973) and neutron (Herbette *et al.*, 1985) diffraction measurements, yielding electron-density profiles perpendicular to the plain of the membrane. Greater detail was subsequently derived from electron diffraction of bidimensionally ordered arrays of ATPase molecules (Taylor *et al.*, 1986; Stokes and Green, 1990), indicating that the globular domain extends 65 Å above the plane of the membrane, and includes a pear-shaped head (65 × 40 × 50Å) and a stalk of 16 Å height and 28 Å diameter. In the early model shown in Fig. 4A the proximity of the ATPase polypeptide chains within the membrane plane is emphasized, as well as the shape of the globular head and stalk protruding from the membrane-bound region.

Useful information regarding the spatial relationships of reference points within the protein structure was obtained by measurements of fluorescence resonance energy transfer indicating a distance greater than 60 Å between lipophilic labels of the membrane bilayer and a fluorescein isothiocyanate (FITC) label of Lys515 (Gutierrez-Merino *et al.*, 1987). Furthermore, Fluorescent labels of Cys670 and 674 with iodoacetamide-directed probes (Squier *et al.*, 1987), and of Cys344 and 364 (bracketing the phosphorylation site) with maleimide-directed probes (Bigelow and Inesi, 1991), appear to be closer to each other than to the fluorescein isothiocyanate of Lys515. This suggests that the alternating helices and beta sheets of the extramembranous portion of the enzyme are bent over. Thereby the Cys 344 and 364 labels and the Cys 670 and 674 labels are approximated while retaining a larger distance from the Lys515 label (Bigelow and Inesi, 1991). These measurements suggest a trigonal structure of the extramembranous domain (Fig. 4B) including nucleotide binding and phosphorylation sites. A reference of this trigonal structure to the membrane bilayer is provided by the estimated distances of 36–40 Å from one of the maleimide labels to troptophans at the membrane interface (Bigelow and Inesi, 1991), and 36–40 Å between the iodoacetamide labels and the same tryptophan residues at the membrane interface (Gryczinski *et al.*, 1989).

With respect to the transmembrane domain, it is likely that the four amphiphilic helices containing the six residues involved in Ca^{2+} binding functions (Fig. 2) are clustered to provide optimal positioning of these residues for Ca^{2+} binding. This arrangement could provide a channel for selective translocation of Ca^{2+} across the membrane, under long-range control by the catalytic domain (Inesi and Kirtley, 1990). A molecular graphics representation of the postulated channel is shown in Fig. 5, demonstrating the spacial relationship of the four acidic groups (Glu 309, Glu771, Asp800, and Glu908) with a dehydrated Ca^{2+}. The internal size of the channel is such that it is possible to move Ca^{2} without major interactions, except at the level of the residues involved in Ca^{2+} binding. It is reasonable to assume that other cation-transport ATPase have their transmembrane helices clustered in a similar way favoring binding and translocation of their specific cations.

Although the graphic representation of Fig. 5 permits a useful appreciation of ligand and segmental protein interaction, as well as general features of a channel of this type, there is no firm evidence defining the number of helices involved in the channel, and whether the helices forming a single channel derive from a single or two complementary 110,000 MW chains. The exact spatial relationships of the helices, and the distinct location of the two (rather than one) Ca^{2+} ions that are known to bind to each ATPase unit, remain to be defined. Further uncertainty is related to the role of a negative charge cluster in the stalk interposed between the globular extramembranous domain and the membrane domain. The stalk cluster is known

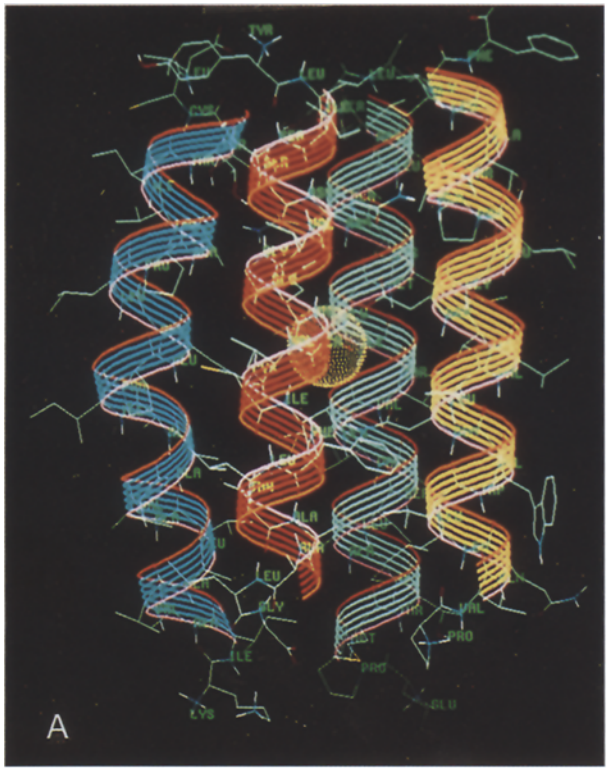
A

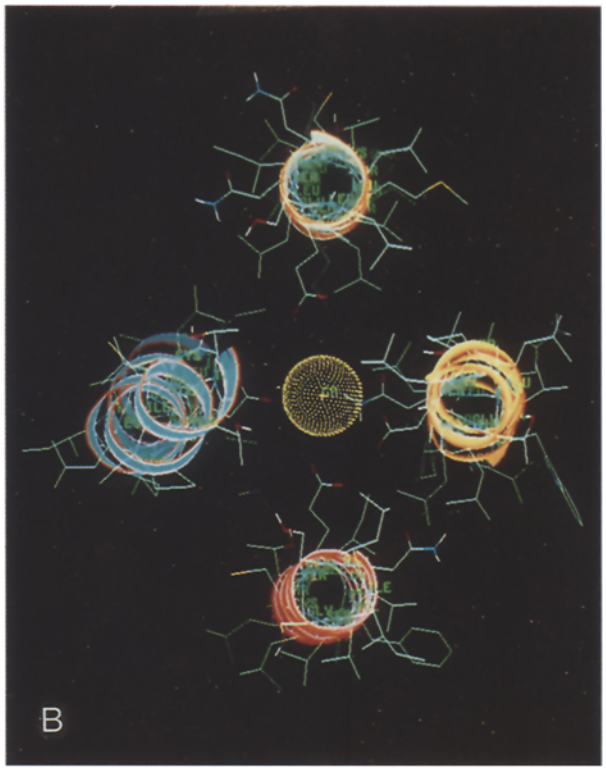
B

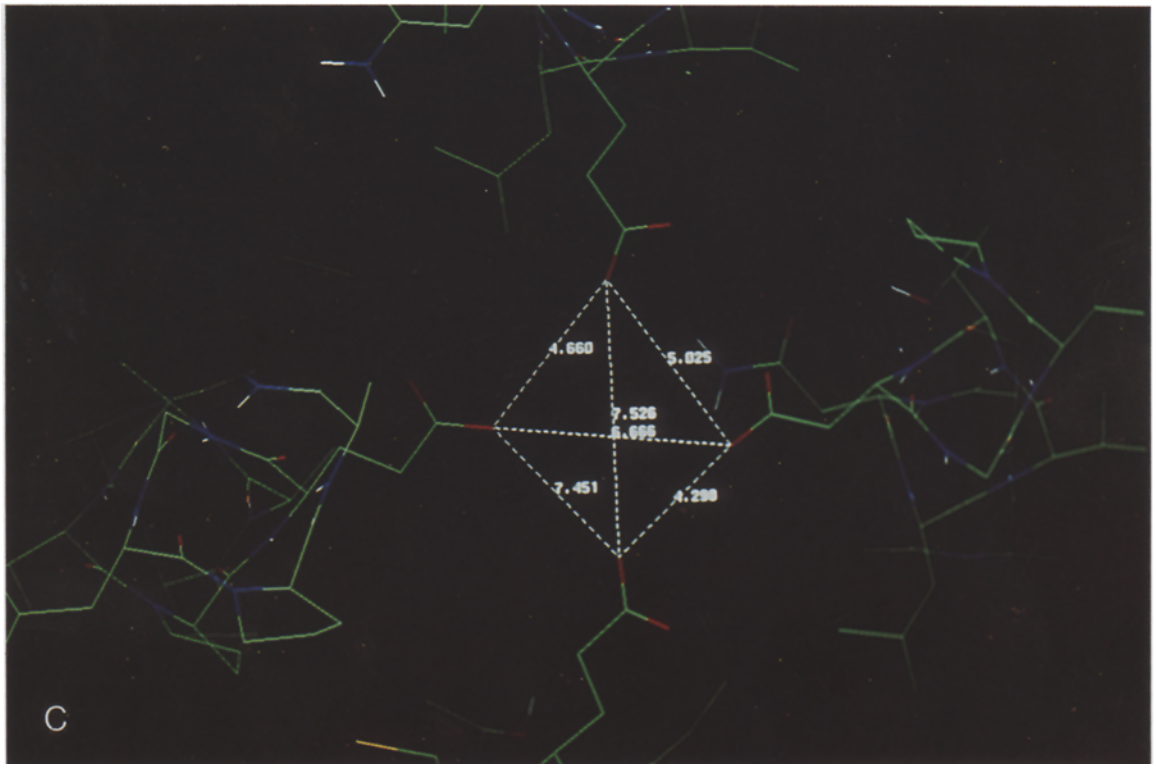
4.660
5.025
7.526
7.451
4.298
C

to bind lanthanides (Squier *et al.*, 1990), but there is no reason to believe that Ca^{2+} binding at this location would occur with functional specificity (Clarke *et al.*, 1989b). It is possible that, as at the opening of the acetylcholine receptor channel (Imoto *et al.*, 1988), the stalk cluster of negative charge in the ATPase stalk may have a role at the opening of the Ca^{2+} channel in selecting ion concentrations in the immediate unstirred solvent layer.

THE STRUCTURAL BASIS OF FUNCTIONAL LINKAGE

From the structural features described so far, it is readily apparent that coupling of catalytic and transport activities requires a long-range functional linkage spanning an approximately 50 Å distance between the phosphorylation site in the extramembranous domain and the cation-binding site within the membrane domain of the ATPase molecule. Therefore, in addition to short-range events related to the chemistry of catalysis, additional effects related to protein conformation are required to explain the long-range linkage of catalytic and cation-binding domains.

It was originally proposed by Mitchell (1957) and Jardetzky (1966) that the vectorial orientation and binding affinity of a cation site may be produced by a single change in conformation of the pump protein. This idea has led to models envisioning the pump protein residing in two major conformational states (E1 and E2, or E and *E) displaying high- or low-affinity cation binding, with different vectorial orientation [for reviews consult Glynn and Karlish (1975); de Meis and Vianna (1979); Forte *et al* (1988)]. The equilibrium between the two states would then be shifted by ligand binding and ATP utilization.

Strong evidence for two conformational states is provided by: (1) the ability of the Ca^{2+}-ATPase to form dimeric crystalline arrays in the absence of Ca^{2+} (Dux and Martonosi, 1983); (2) the total loss of this ability upon addition of Ca^{2+}; and (3) the restoration of this ability following the addition of the specific inhibitor thapsigargin (Sagara and Inesi, 1991) even in the presence of Ca^{2+}. The functional counterpart of the two states is the enzyme's ability to be phosphorylated by ATP (but not by P_i) in the presence of Ca^{2+}, and its ability to be phosphorylated by P_i (but not by ATP) in the absence of Ca^{2+}.

In addition to the conformational effect of Ca^{2+}, another conformational effect is apparently produced by formation of the phosphorylated enzyme intermediate. In fact, enzyme phosphorylation by utilization of ATP in the presence of Ca^{2+}, or by utilization of P_i in the absence of Ca^{2+}, is followed by a change in the association of ATPase molecules within the membrane, as revealed by a reduction of fluorescence resonance energy transfer between appropriate labels placed on distinct ATPase molecules (Watanabe and Inesi, 1982; Bigelow *et al.*, 1992).

It is possible that the Ca^{2+}-induced state and the phosphorylation-induced are predominant during enzyme cycling. An intriguing question is whether there are *only* two conformational states alternating within the catalytic and transport cycle, or whether intermediate states are produced within the sequence of partial reactions of a single cycle (Jencks, 1989). The observation that bound Ca^{2+} is occluded within the ATPase protein, following substrate utilization and preceding vectorial dissociation of Ca^{2+} and cleavage of P_i, suggests that at least one intermediate state is formed (Glynn and Karlish, 1990).

In spite of the different characteristics of distinct enzyme states, no major effects of Ca^{2+} or phosphorylation are detected by measurements of ellipticity or energy transfer within the ATPase molecule (Nakamoto and Inesi, 1986; Bigelow *et al.*, 1992). Therefore, the observed alternation of enzyme conformational states must be produced by changes in tertiary structure, but small or no changes in secondary structure. It is of interest that similar conclusions were recently reached regarding the bacterial aspartate receptor, whose extramembranous ligand-binding domain was crystallized as an active dimer, and its three-dimensional structure determined by x-ray crystallographic methods. It was then shown that the ligand-binding site is located more than 60 Å from the

Fig. 5. Model of a possible channel composed of helices 4, 5, 6, and 8 which contain the Ca^{2+} binding residues. Because of the presence of prolines in the sequences, the helices are bent. The Ca^{2+} residues are arranged facing into the central space at the middle of the helix cluster. A Ca^{2+} ion with van der Waals sphere is shown as a yellow ball in the center of the channel complexed with the Ca^{2+} binding side chains. (A) Side view of channel. (B) View down the channel from the cytosol. (C) View of the Ca^{2+} binding site in the middle of the channel. Four carboxyl groups on the side chains of Ca^{2+}-binding residues are clustered in the center of the channel in position to coordinate with Ca^{2+}.

presumed membrane surface, and that ligand binding produces only small structural changes of the individual subunits, but a definite change in orientation of the subunits relative to each other (Milburn *et al.*, 1991).

Long-range functional linkages extending from extramembranous triggering domains through transmembrane helical clusters may be general features of transmembrane signalling mechanisms. In the cation-transport ATPases, a highly homologous helical segment links the phosphorylation and the cation-binding domains. It is likely that this segment provides the structural means for functional linkage between the two domains within the ATPase protein.

REFERENCES

Bastide, F., Meissner, G., Fleischer, S., and Post, R. L. (1973). *J. Biol. Chem.* **248**, 8385–8391.

Bigelow, D. J., and Inesi, G. (1991). *Biochemistry* **30**, 2113–2125.

Bigelow, D. J., Squier, T. C., and Inesi, G. (1992). *J. Biol. Chem.*, in press.

Brandl, C. J., Green, N. M., Korczak, B., and MacLennan, D. H. (1986). *Cell* **44**, 597–607.

Burk, S. E., Lytton, J., MacLennan, D. H., and Shull, G. E. (1989). *J. Biol. Chem.* **264**, 18561–18568.

Campbell, A. M., Kessler, P. D., Sagara, Y., Inesi, G., and Fambrough, D. M. (1991). *J. Biol. Chem.* **266**, 16050–16055.

Clarke, D. M., Loo, T. W., Inesi, G., and MacLennan, D. H. (1989a). *Nature (London)* **339**, 476–478.

Clarke, D. M., Maruyama, K., Loo, T. W., Leberer, E., Inesi, G., and MacLennan, D. H. (1989b). *J. Biol. Chem.* **264**, 11246–11251.

DeAncos, J., and Inesi, G. (1988). *Biochemistry* **27**, 1793–1803.

Deamer, D., and Baskin, R. (1969). *J. Cell Biol.* **42**, 296–307.

De Meis, L., and Vianna, A. (1979). *Annu. Rev. Biochem.* **48**, 275–292.

Degani, C., and Boyer, P. D. (1973). *J. Biol. Chem.* **248**, 8222–8226.

Dupont, Y., Harrison, S., and Hasselbach, W. (1973). *Nature (London)* **244**, 554–558.

Dux, L., and Martonosi, A. (1983). *J. Biol. Chem.* **258**, 10111–10115.

Eggermont, J. A., Wuytack, F., DeJaegere, S., Nelles, L., and Casteels, R. (1989). *Biochem. J.* **260**, 757–761.

Eggermont, J. A., Wuytack, F., Verbist, J., and Casteels, R. (1990). *Biochem. J.* **271**, 649–653.

Forte, J. G., Forte, G. M., and Saltman, P. (1988). *J. Cell Phys.* **293**, 304.

Glynn, I. M., and Karlish, S. J. D. (1975). *Annu. Rev. Physiol.* **37**, 13–55.

Glynn, I. M., & Karlish, S. J. D. (1990). *Annu. Rev. Biochem.* **59**, 171–205.

Greeb, J., and Shull, G. E. (1989). *J. Biol. Chem.* **264**, 18569–18576.

Gryczynski, I., Wiczk, W., Inesi, G., Squier, T. C., and Lakowicz, J. R. (1989). *Biochemistry* **28**, 3490–3498.

Gunteski-Hamblin, A.-M., Greeb, J., and Shull, G. E. (1988). *J. Biol. Chem.* **263**, 15032–15040.

Gutíerrez-Merino, C., Munkonge, F. M., Mata, A. M., East, J. M., Levinson, B. L., Napier, R. M., and Lee, A. G. (1987). *Biochim. Biophys. Acta* **897**, 207–216.

Herbette, L. G., DeFoor, P., Fleischer, S., Paolini, P., Scarpa, A., and Blasie, J. K. (1985). *Biochim. Biophys. Acta* **817**, 103–122.

Imoto, K., Busch, C., Sakmann, B., Mishina, M., Konno, T., Nakai, J., Bujo, H., Mori, Y., Fukuda, K., and Numa, S. (1988). *Nature (London)* **335**, 645–648.

Inesi, G., and Asai, H. (1968). *Arch. Biochem. Biophys.* **126**, 469–477.

Inesi, G., and Kirtley, M. E. (1990). *J. Membr. Biol.* **116**, 1–8.

Inesi, G., Sumbilla, C., and Kirtley, M. E. (1990). *Physiol. Rev.* **70**, 749–760.

Inesi, G., Lewis, D., Nikic, D., Hussain, A., and Kirtley, M. E. (1992). *Adv. Enzymol.*, **65**, 185–215.

James, P., Inui, M., Tada, M., Chiesi, M., and Carafoli, E. (1989a). *Nature (London)* **342**, 90–92.

James, P. H., Pruschy, M., Vorherr, T. E., Penniston, J. T., and Carafoli, E. (1989b). *Biochemistry* **28**, 4253–4258.

Jardetzky, O. (1966). *Nature (London)* **211**, 969–970.

Jencks, W. P. (1989). *J. Biol. Chem.* **264**, 18855–18858.

Kaprielian, Z., Campbell, A. M., and Fambrough, D. M. (1989). *Mol. Brain Res.* **6**, 55–60.

Karin, N. J., Kaprielian, Z., and Fambrough, D. M. (1989). *Mol. Cell. Biol.* **9**, 1978–1986.

Kawakami, K., Nojima, H., Ohta, T., and Nagano, K. (1986). *Nucleic Acids Res.* **14**, 2833–2844.

Kirtley, M. E., and Inesi, G. (1992). In *Structure and Function of Biological Membranes* (Yeagle, P., ed.), Telford Press, Caldwell, New Jersey, pp. 893–914.

Korczak, B., Zarain-Herzberg, A., Brandl, C. J., Ingles, C. J., Green, N. M., and MacLennan, D. H. (1988). *J. Biol. Chem.* **263**, 4813–4819.

Lompre, A. M., De La Bastie, D., Boheler, K. R., and Schwartz, K. (1989). *FEBS Lett.* **249**, 35–41.

Lytton, J., and MacLennan, D. H. (1988). *J. Biol. Chem.* **263**, 15024–15031.

Lytton, J., Zarain-Herzberg, A., Periasamy, M., and MacLennan, D. H. (1989). *J. Biol. Chem.* **264**, 7059–7065.

MacLennan, D. H., Brandl, C. J., Korczak, B., and Green, N. M. (1985). *Nature (London)* **316**, 696–700.

Maeda, M., Ishizaki, J., and Futai, M. (1988). *Biochem. Biophys. Res. Commun.* **157**, 203–209.

Maeda, M., Oshiman, K. I., Tanura, S., and Futai, M. (1990). *J. Biol. Chem.* **265**, 9027–9032.

Makinose, M. (1969). *Eur. J. Biochem.* **10**, 74–82.

Milburn, M. V., Privé, G. G., Milligan, D. L., Scott, W. G., Yeh, J., Jancarik, J., Koshland, D. E., Jr., and Kim, S.-H. (1991). *Science* **254**, 1342–1347.

Mitchell, P. (1957). *Nature (London)* **180**, 134–136.

Mitchinson, C., Wilderspin, A., Trinnaman, B. J., and Green, N. M. (1982). *FEBS Lett.* **146**, 87–92.

Nakamoto, R. K., and Inesi, G. (1986). *FEBS Lett.* **194**, 258–262.

Palmero, I., and Sastre, L. (1989). *J. Mol. Biol.* **210**, 737–748.

Pick, U., and Karlish, S. J. (1980). *Biochim. Biophys. Acta* **626**, 255–261.

Reuben, M. A., Lasater, L. S., and Sachs, G. (1990). *Proc. Natl. Acad. Sci. USA* **87**, 6767–6771.

Sagara, Y., and Inesi, G. (1991). *J. Biol. Chem.* **266**, 13503–13506.

Serrano, R., Kielland-Brandt, M. C., and Fink, G. R. (1986). *Nature (London)* **319**, 689–693.

Shull, G. E., and Greeb, J. (1988). *J. Biol. Chem.* **263**, 8646–8657.

Shull, G. E. and Lingrel, J. B. (1986). *J. Biol. Chem.* **261**, 16788–16791.

Shull, G. E., Schwartz, A., and Lingrel, J. B. (1985). *Nature (London)* **316**, 691–695.

Shull, G. E., Greeb, J., and Lingrel, J. B. (1986). *Biochemistry* **25**, 8125–8132.

Squier, T. C., Bigelow, D. J., Garcia de Ancos, J., and Inesi, G. (1987). *J. Biol. Chem.* **262**, 4748–4754.
Squier, T. C., Bigelow, D. J., Fernandez-Belda, F. J., De Meis, L., and Inesi, G. (1990). *J. Biol. Chem.* **265**, 13713–13720.
Stokes, D. L., and Green, N. M. (1990). *J. Mol. Biol.* **213**, 529–538.
Strehler, E. E., Strehler-Page, M.-A., Vogel, G., and Carafoli, E. (1989). *Proc. Natl. Acad. Sci. USA* **86**, 6908–6912.
Strehler, E. E., James, P., Fischer, R., Heim, R., Vorherr, T., Filoteo, A. G., Penniston, J. T., and Carafoli, E. (1990). *J. Biol. Chem.* **265**, 2835–2842.
Sumbilla, C., Cantilina, T., Collins, J. H., Malak, H., Lakowicz, J. R., and Inesi, G. (1991). *J. Biol. Chem.* **266**, 12682–12689.
Taylor, W. R., and Green, N. M. (1989). *Eur. J. Biochem.* **179**, 241–248.
Taylor, K. A., Dux, L., and Martonosi, A. (1986). *J. Mol. Biol.* **187**, 417–427.
Verma, A. K., Filoteo, A. G., Stanford, D. R., Wieben, E. D., Penniston J. T., Strehler, E. E., Fischer, R., Heim, R., Vogel, G., Mathews, S., Strehler-Page, M.-A., James, P., Vorherr, T., Krebs, J., and Carafoli, E. (1988). *J. Biol. Chem.* **263**, 14152–14159.
Watanabe, T., and Inesi, G. (1982). *Biochemistry* **21**, 3254–3259.
Yamamoto, T., and Tonomura, Y. (1968). *J. Biochem. (Tokyo)* **64**, 137–145.